Electro-capillary instability of a nematic-isotropic interface

Patrick Oswald

A Letters Journal Exploring the Frontiers of Physics

OFFPRINT

Electro-capillary instability of a nematic-isotropic interface

P. Oswald

EPL, **90** (2010) 16005

A Letters Journal Exploring the Frontiers of Physics

April 2010

EPL, **90** (2010) 16005
doi: 10.1209/0295-5075/90/16005

www.epljournal.org

Electro-capillary instability of a nematic-isotropic interface

P. Oswald[(a)]

Université de Lyon, Ecole Normale Supérieure de Lyon, Laboratoire de Physique, UMR 5672 of the CNRS 46 Allée d'Italie, 69364 Lyon Cedex 07, France, EU

received 26 February 2010; accepted in final form 25 March 2010
published online 3 May 2010

PACS 61.30.Hn – Surface phenomena: alignment, anchoring, anchoring transitions, surface-induced layering, surface-induced ordering, wetting, prewetting transitions, and wetting transitions
PACS 47.20.Ma – Interfacial instabilities (*e.g.*, Rayleigh-Taylor)
PACS 47.65.-d – Magnetohydrodynamics and electrohydrodynamics

Abstract – We have studied the morphological instability under AC electric field of a nematic-isotropic interface confined between two electrodes set at different temperatures. The electrodes are treated for homeotropic anchoring so that, when the field is increased, the Ericksen elastic stress vanishes. In this limit, the instability resembles that observed in ordinary liquids. However, significant differences were observed.

Introduction. – In 1974, de Gennes [1] showed that the free surface of a nematic liquid crystal can destabilize into a hill-and-valley structure when the director field is distorted by a strong enough magnetic field. In the example treated by de Gennes, the critical field and the wavelength at the onset of the instability resulted from the competition between the destabilizing action of the Ericksen elastic stress and the stabilizing effect of the capillary and gravitational forces. This instability and another one of the same type, which led to an undulation of the interface, were observed a few years later at the nematic-isotropic (N-I) interface [2–4].

Similarly, the interface between two isotropic fluids having different electrical properties can become unstable under the action of an electric field. In this case, the Maxwell electric stress (absent in the de Gennes calculation, but taken into account in the work of Yokoyama *et al.* [3]) is destabilizing, whereas gravity and surface tension are stabilizing [5,6].

We found that an instability similar to that observed in usual liquids can develop at a N-I interface of a liquid crystal of positive dielectric anisotropy when the Ericksen elastic stress vanishes. A sketch of our experiment is shown in fig. 1. The liquid crystal is sandwiched between two parallel electrodes that had been treated for homeotropic anchoring. The N-I interface is prepared in a temperature gradient and is subjected to a strong AC electric field. "Strong" means that the field is large enough to break the oblique anchoring [7] of the molecules at the interface. In this limit, the Ericksen elastic stress vanishes because the director aligns parallel to the electric field, and the elastic de Gennes-type instability disappears. On the other hand, the interface is still strongly stressed by the electric field and can destabilize under its sole action.

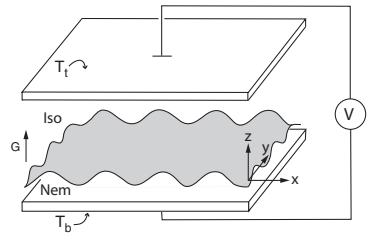

Fig. 1: Schematic view of the experimental device. T_b and T_t are the temperatures displayed by the two circulating bathes and G is the temperature gradient proportional to $\Delta T = T_t - T_b$.

Although this experiment resembles those with isotropic liquids, there are significant differences between them. Indeed, the surface tensions are very different: while $\gamma \sim 0.02$–$0.08\,\mathrm{J/m^2}$ at the interface between two immiscible liquids, $\gamma \sim 10^{-5}\,\mathrm{J/m^2}$ at the N-I interface [7]. The small value of the surface tension is due in this case to the weakly first-order nature of the N-I transition [8]. Another important difference lies in the fact that the two phases coexist and can transform into each other. This phase equilibrium must be taken into account at the interface. This point was not discussed in the previous work carried out by Yokoyama *et al.* [3]. Finally, we imposed a

(a) E-mail: patrick.oswald@ens-lyon.fr

temperature gradient in order to prepare a planar interface. The latter has a stabilizing effect and should act like gravity does in thick fluid layers. The advantage here is that the temperature gradient can be easily tuned contrary to gravity, allowing us to study its effect in detail. It should be noted that gravity is completely insignificant in our problem because the two phases have very similar densities: $\Delta\rho/\rho \sim 10^{-3}$ [9].

The experiment which was carried out is described in the next section. Our results on the onset of instability and the wavelength evolution as a function of the electric field and the temperature gradient are given in the third section. In the fourth section, we extend the classical EHD model to the nematic case by taking into account the nematic anisotropy and the phase equilibrium at the interface. Our experimental data are then compared to the theoretical predictions. Finally, perspectives are drawn in the last section.

Experimental procedure. – In order to observe the nematic-isotropic interface we prepared 30 μm thick layers of 4-*n*-octyl-cyanobiphenyl (8CB, nematic range 33–41 °C) between two ITO-coated glass plates of dimensions $25 \times 25 \times 1$ mm. On each plate, the ITO was partly removed so that only a 5 mm $\times$ 5 mm square in the center of the sample was submitted to the electric field. The liquid crystal was purchased from Merck and used without further purification. Its freezing range at the N-I transition is very narrow, of the order of 0.02 K. The two electrodes were treated for strong homeotropic anchoring by spin-coating a thin layer of polyimide 0626 from Nissan (diluted to 3% in weight in solvent 26 from Nissan). The later was dried for one hour at 80 °C and was then polymerized for one hour at 160 °C. The sample was sandwiched between two transparent ovens which were separately regulated in temperature thanks to two circulating bathes (for a description of the setup, see [10]). A polarizing microscope and a video camera allowed us to observe the sample and to capture images with a resolution of 1380×1024 pixels. A HP 3325B function generator, amplified by a TREK PZD700 amplifier, was used to impose an electric field to the sample. The charge relaxation frequency f_c of the samples was measured with a HP 4284A precision LCR meter. We found that in all samples, $f_c \approx 80$–100 Hz in the isotropic liquid. The thickness of the nematic layer was obtained from cell capacitance measurements in the dielectric regime (in practice at 10 kHz). Figure 2 shows the cell capacitance measured at low and large voltages (0.1 Vrms and 10 Vrms, respectively) as a function of the average sample temperature $\langle T\rangle = (T_b + T_t)/2$. While the curve at 0.1 Vrms is discontinuous, that at 10 Vrms is continuous. The discontinuity of the capacitance curve at 0.1 Vrms marks the formation of the N-I interface and indicates that the director field is no more homeotropic because of the oblique anchoring of the molecules at the interface [7]. By contrast, the oblique anchoring is overcome at a voltage V_a above which the director aligns

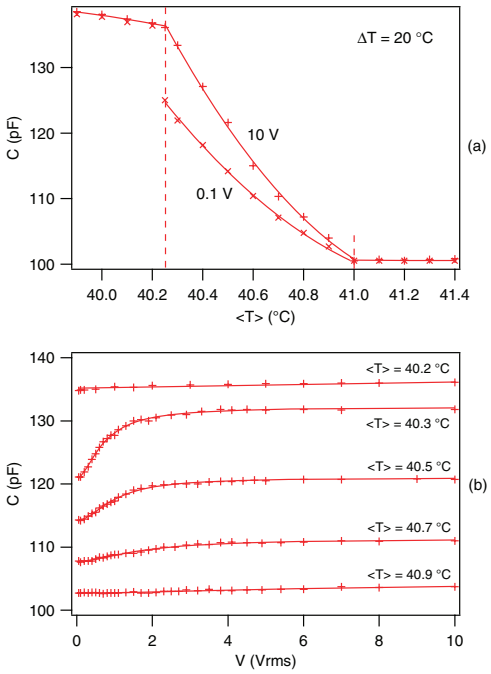

Fig. 2: (Colour on-line) (a) Cell capacitance as a function of the average temperature measured at 0.1 Vrms and 10 Vrms. Note the two phases coexist over a temperature interval of 0.75 °C. (b) Cell capacitance as a function of the applied voltage measured at various average temperatures. For the two graphs, $\Delta T = 20$ °C and $f = 10$ kHz (dielectric regime). Lines are just guides for the eyes.

everywhere parallel to the electric field. Experimentally, $V_a \approx 4$ Vrms (see fig. 2(b)). Writing that at V_a the electric correlation length $\sqrt{\frac{K}{\varepsilon_a \varepsilon_0}}\frac{1}{E}$ is equal to the anchoring penetration length $\frac{K}{W_a}$ yields

$$V_a \sim \frac{W_a d}{\sqrt{K \varepsilon_0 \varepsilon_a}}, \tag{1}$$

where K is the bend constant, W_a the anchoring energy [7,8], ε_0 the permittivity of the free space and $\varepsilon_a = \varepsilon_{\parallel} - \varepsilon_{\perp}$ the dielectric anisotropy of the nematic phase at the transition. With the values $K \approx 2 \cdot 10^{-12}$ N [11], $\varepsilon_a \approx 4$ [12], eq. (1) gives $W_a \sim 10^{-6}$ J/m^2 rad^2 in satisfactory agreement with previous measurements of Faetti and Palleschi [7]: $W_a \approx 8.5 \cdot 10^{-7}$ J/m^2 rad^2. As for the thickness h of the nematic layer, it is simply given by formula

$$h = \frac{1 - C_I/C}{1 - C_I/C_{\parallel}} d, \tag{2}$$

with d being the sample thickness (30 ± 1 μm in all experiments) and C the plateau capacitance measured at 10 Vrms, and which decreases from $C_{\parallel}$ in the nematic phase down to C_I in the isotropic liquid. This method yields h to within ± 1 μm.

Experimental results. – The experiment showed that the front becomes unstable and starts to undulate by forming a stationary hexagonal array when the electric

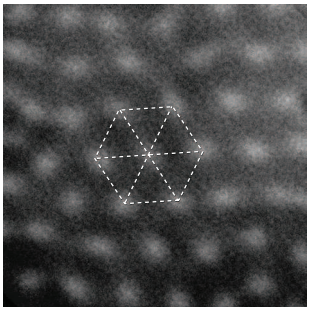

Fig. 3: Photograph in natural light of the N-I interface at the onset of instability. The contrast has been greatly enhanced for better visualization of the hexagonal array. The side length of the hexagon is 50 μm. $h = 19\,\mu$m, $\langle T \rangle = 40.1\,^\circ$C, $\Delta T = 40\,^\circ$C, $V = 27.8$ Vrms and $f = 100$ kHz.

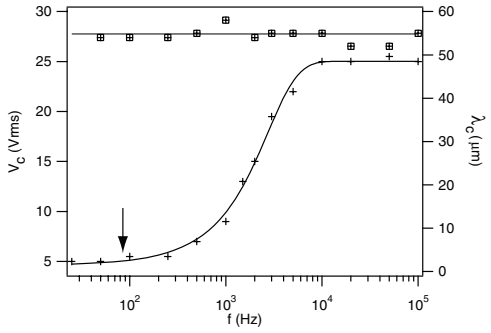

Fig. 4: Critical voltage and critical wavelength as a function of the frequency. $h = 19\,\mu$m, $\langle T \rangle = 40.1\,^\circ$C and $\Delta T = 40\,^\circ$C. The arrow indicates the charge relaxation frequency.

field is increased (fig. 3). This instability is not due to convection because no fluid flow was detected in the microscope. This bifurcation is supercritical, the growth time of the undulation diverging at the onset of instability. The critical voltage V_c depends on the frequency f of the electric field, contrary to the critical wavelength λ_c of the modulation which is approximately constant (fig. 4). More precisely, V_c is constant in the conducting regime at low frequency ($f < f_c$) and at high frequency ($f > 100 f_c$) where its value is typically 5 times larger than at low frequency. In this limit known as the "dielectrophoretic limit" [13], the frequency is high enough to make all free charge effects insignificant in the bulk, but also at the interface. Note that the passage between these two regimes takes place over two decades in frequency. This behavior is compatible with recent numerical simulations of the destabilization of fluids layers subjected to an AC electric field [14].

Because the calculations are easier in the dielectrophoretic limit (only polarization charges have to be considered) we did all our measurements in this regime (in practice at 10 kHz). Figure 5 shows a few pictures taken above the onset of instability immediately after the voltage has been applied and the pattern has been formed. Experiment shows that the hexagonal array which develops

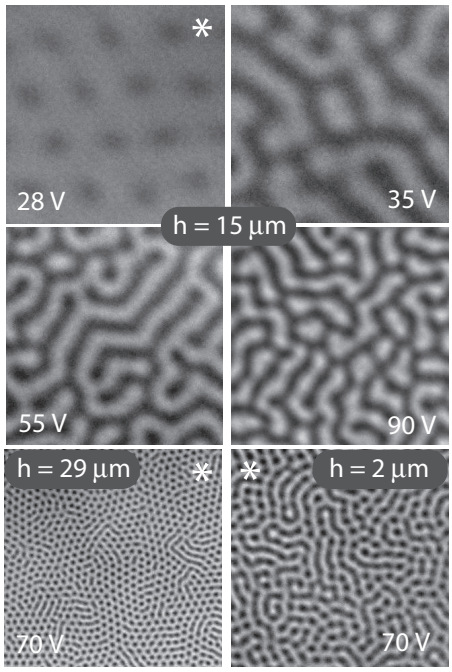

Fig. 5: Photos in natural light of the N-I interface taken just after the application of the electric field. The contrast has been enhanced for better visualization of the patterns. The voltage is given in Vrms. Photos labeled with a star have been taken close to the onset of instability. Each photo is 200 μm $\times$ 200 μm in dimension. $\Delta T = 40\,^\circ$C.

at the onset of instability is progressively replaced by a disordered band structure when the voltage V is increased. This new labyrinth pattern is very similar to the one which was observed by Schäffer *et al.* in very thin polymer layers destabilized by an electric field [15,16]. The passage at increasing V from a hexagonal array to a labyrinth pattern depends on the temperature gradient and also on the thickness of the nematic layer. This point will be detailed in a separate article. Here we just emphasize that a small temperature gradient G or a large h favor the formation of the hexagons over the bands. In order to quantify our results, we then measured the characteristic wavelength λ of the patterns close to the onset of instability (typically for $V_c < V < 2V_c$). It was obtained by calculating the 2D Fourier transform of each image (the latter displays a ring with the radius being inversely proportional to the wavelength). Figure 6(a) shows that for a given temperature gradient ($\Delta T = 40\,^\circ$C), λ decreases when h increases at constant V and when V increases at constant h. As for the role of the temperature gradient, it is shown in fig. 6(b). These data show that λ tends to increase at constant h and V when the temperature gradient is increased (λ increases to about 30% when ΔT is raised from 10 to 40 °C with no clear tendency between 10 and 20 °C). We also measured the critical voltage V_c as a function of h for three different ΔT (fig. 7). The result is that V_c increases when ΔT increases and when $h \to 0$ or d. In other words, the interface is more stable when it is close to a plate and when the temperature gradient is important.

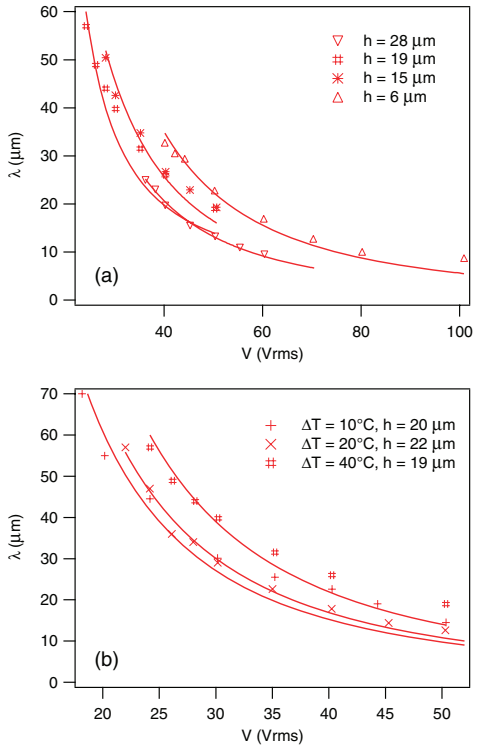

Fig. 6: (Colour on-line) Wavelength as a function of the applied voltage: (a) measurements at different thicknesses h and fixed temperature gradient ($\Delta T = 40\,^{\circ}\mathrm{C}$); (b) measurements at different temperature gradients but similar thicknesses ($h \approx 20\,\mu\mathrm{m}$). Solid lines are the best fits to a $1/V^2$ law (eq. (9)).

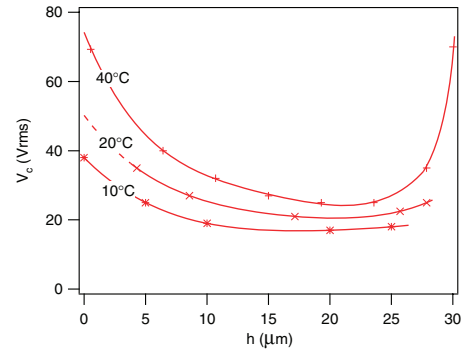

Fig. 7: (Colour on-line) Critical voltage as a function of the thickness of the nematic layer. The value of ΔT is indicated beside each curve. The lines are just guides for the eye.

How to model the instability? – In this section, to simplify the calculations, we assume that all the thermal conductivities in the nematic phase and in the isotropic liquid are equal ($\kappa_{\parallel} = \kappa_{\perp} = \kappa_I = \kappa$). In this case, the temperature gradient inside the sample is constant, independent of the shape of the interface and given by $G = \frac{\kappa_g}{\kappa}\frac{\Delta T}{4e}$ by denoting by κ_g the glass conductivity (of the order of 5κ [8]) and by $4e$ the total thickness of the glass plates (in practice, four glass plates of thickness $e = 1\,\mathrm{mm}$) [10].

We shall first consider the phase equilibrium below the onset of instability. Without electric field, the interface temperature must be equal to the transition temperature T_{NI} (within a very small correction less than a mK due to the distortion of the director field) and the thickness of the nematic layer is simply given by $h = (T_{NI} - T_{-})/G$ by denoting by T_{-} the temperature of the bottom electrode in contact with the liquid crystal. When an electric field is applied, the interface temperature changes and becomes T_i. This new equilibrium temperature is obtained by minimizing the total free energy [17]:

$$F = \int_0^h -S_N(T - T_{NI})\mathrm{d}z + \int_h^d -S_I(T - T_{NI})\mathrm{d}z - \int_0^h \frac{\vec{E}_N\vec{D}_N}{2}\mathrm{d}z - \int_h^d \frac{\vec{E}_I\vec{D}_I}{2}\mathrm{d}z + \gamma(\theta). \quad (3)$$

In this formula, indices N and I stand for nematic and isotropic, respectively, S is the volume entropy at temperature T_{NI}, $\vec{E}$ is the electric field, $\vec{D} = \varepsilon_0\underline{\varepsilon}\vec{E}$ is the electric displacement and $\gamma(\theta)$ is the surface energy (with θ the angle between the director and the normal to the interface). If $V > V_a$, $\theta = 0$ and $\gamma(\theta) = \gamma(0) = \mathrm{const}$. A straightforward calculation in this limit gives

$$F = \Delta S\left(T_{-}h + G\frac{h^2}{2} - T_{NI}h\right) - \frac{1}{2}\frac{\varepsilon_0\varepsilon_I\varepsilon_{\parallel}V^2}{\varepsilon_I h + \varepsilon_{\parallel}(d-h)} + \mathrm{const}, \quad (4)$$

where $\Delta S = S_I - S_N$ is the entropy jump at the transition and ε_I (respectively, $\varepsilon_{\parallel}$) the dielectric constant of the isotopic liquid (respectively, of the nematic phase parallel to the director). At equilibrium, the energy is stationary: $\partial F/\partial h = 0$. This yields the interface temperature $T_i = T_{-} + Gh$:

$$\frac{T_i - T_{NI}}{T_{NI}} = \frac{\epsilon_0\varepsilon_I\varepsilon_{\parallel}(\varepsilon_{\parallel} - \varepsilon_I)V^2}{2\Delta H[\varepsilon_I h + \varepsilon_{\parallel}(d-h)]^2}, \quad (5)$$

where $\Delta H = T_{NI}\Delta S$ is the latent heat per unit volume. Because $\varepsilon_{\parallel} > \varepsilon_I$, $T_i > T_{NI}$. As expected, the electric field favors the nematic phase over the isotropic liquid. For our experiment, we calculate $T_i - T_{NI} \approx 7\,\mathrm{mK}$ at $V = 50\,\mathrm{Vrms}$ by taking $\varepsilon_I = 9$, $\varepsilon_{\parallel} = 12$ [12], $\Delta H = 1.5 \cdot 10^6\,\mathrm{J/m^3}$ [8] and $h = d/2 = 15\,\mu\mathrm{m}$. This corresponds to a small front displacement δh in the cell gap of the order of $0.3\,\mu\mathrm{m}$ at $\Delta T = 20\,^{\circ}\mathrm{C}$. In practice, we were not able to detect this displacement except when the front started to touch the upper electrode ($h \approx d$): in this case, we observed that a strong electric field favored the wetting of the nematic phase, meaning that h was slightly increasing in agreement with the calculation.

The situation becomes more complicated above the onset of instability when the front buckles into a sinusoidal shape of equation $u = u_0\sin(kx)$ centered around the isotherm of temperature T_i. In this case, the electric

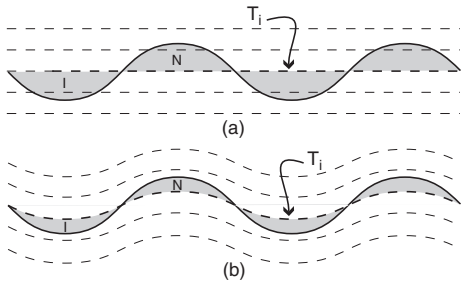

Fig. 8: When the front buckles in the temperature gradient, regions of overheated nematic and undercooled isotropic liquid develop on both sides of the isotherm of temperature T_i (shaded areas). The dashed lines are the isotherms. In (a) the isotherms are assumed to be flat; in (b) they undulate with the interface. This leads to a reduction of the surface area of the shaded regions.

field must be calculated at second order in u_0 by solving the bulk equations $\mathrm{curl}\,\vec{E}=0$ and $\mathrm{div}\,\vec{D}=0$ with the requirement that the tangential component of the electric field and the normal component of the electric displacement be continuous at the interface. A direct calculation using Mathematica shows that the total energy changes by an amount $\delta F=\frac{1}{4}f(k,U,G)u_0^2$, where

$$f(k,V,G)=\frac{\Delta H}{T_{NI}}G+\gamma k^2 - \frac{k\varepsilon_0\varepsilon_I\varepsilon_\parallel(\varepsilon_\parallel-\varepsilon_I)^2V^2}{[\varepsilon_I h+\varepsilon_\parallel(d-h)]^2[\varepsilon_\parallel\tanh[k(d-h)]+\epsilon_I\tanh(kh)]}. \quad (6)$$

In this equation, γ is the surface tension of the N-I interface (which we assume to be constant because we are well below the critical point [18]). In this calculation, we assumed that the director was everywhere aligned along the electric-field direction in the nematic phase which, consequently, behaves as an isotropic liquid of dielectric constant $\varepsilon_\parallel$. This hypothesis is quite well verified because the electric correlation length is always very small in comparison with the wavelength and the thickness of the nematic layer. Three terms appear in this equation:

1) The first one, proportional to G, corresponds to the volume free energy excess of the overheated nematic and the undercooled isotropic liquid which nucleated on both sides of the isotherm at temperature T_i (fig. 8(a)). This term reflects the stabilizing effect of the temperature gradient and it is important at all wavelengths.

2) The second term is simply the excess of surface free energy: it mainly stabilizes the short wavelengths.

3) The third term (calculated in a different way by Onuki [19]) represents the gain in electric energy caused by the distortions of the electric field lines when the interface undulates: this is the destabilizing term responsible for the instability.

If h and $d-h$ are large enough, *i.e.* if the interface is not very close to an electrode, then the tanh terms in eq. (6) are close to 1. In this limit, the calculation predicts that the interface destabilizes above a critical voltage V_c given by

$$V_c^2=\frac{2[h\varepsilon_I+(d-h)\varepsilon_\parallel]^2(\varepsilon_\parallel+\varepsilon_I)}{\varepsilon_0\varepsilon_I\varepsilon_\parallel(\varepsilon_\parallel-\varepsilon_I)^2}\sqrt{\frac{\gamma G\Delta H}{T_{NI}}} \quad (7)$$

with the critical wavelength

$$\lambda_c=\frac{2\pi}{k_c}=2\pi\sqrt{\frac{T_{NI}\gamma}{G\Delta H}}. \quad (8)$$

These two formulas predict that V_c increases and λ_c decreases when G increases, in qualitative agreement with experiments. On the other hand, eq. (7) does not predict the good shape of the curve $V_c(h)$ nor the good order of magnitude for the critical voltage: indeed, by taking $\varepsilon_\parallel=12$, $\varepsilon_\perp=7$ and $\varepsilon_I=9$ [12], $\gamma=10^{-5}\,\mathrm{J/m^2}$ [7] and $\Delta T=40\,^\circ\mathrm{C}$ ($G\approx 5\cdot10^4\,^\circ\mathrm{C/m}$ (see footnote[1])) this equation gives $V_c=154\,\mathrm{Vrms}$ for $h=d/2$ whereas experiment gives $V_c\approx 25\,\mathrm{Vrms}$. The same holds for the wavelength, eq. (8) leading to $\lambda_c=1.3\,\mu\mathrm{m}$ instead of the $60\,\mu\mathrm{m}$ observed experimentally (fig. 6).

This large quantitative disagreement indicates that the stabilizing effect of the temperature gradient is very strongly overestimated in our simplified model. This could be due to the fact that the distortion of the interface distorts the isotherms inside the sample (fig. 8(b)), the three thermal conductivities, $\kappa_\perp$ and $\kappa_\parallel$ in the nematic phase and κ_I in the isotropic liquid, being all different. In addition, the director field should not be strictly homeotropic since the director must align parallel to the electric field at large field. This distortion of the director field could focus the heat inside the nematic phase, an effect which is well known to considerably decrease the onset of Rayleigh-Bénard instability in nematics [8]. In addition, we cannot exclude local heating effects, even if we have no direct experimental evidence about their existence.

It is nevertheless interesting to note that the combination $\frac{\lambda_c V_c^2}{[h\varepsilon_I+(d-h)\varepsilon_\parallel]^2}$ must be independent of the stabilizing thermal term in $G\Delta H$, that we failed to calculate in the free energy, as it is equal to $\gamma\frac{4\pi(\varepsilon_\parallel+\varepsilon_I)}{\varepsilon_0\varepsilon_I\varepsilon_\parallel(\varepsilon_\parallel-\varepsilon_I)^2}$ according to eqs. (7) and (8). To check this point, we reported this quantity as a function of λ_c in fig. 9. As we can see in this figure, it is a constant within the dispersion of the data. From its average value, $0.35\pm0.1\,\mathrm{V^2/\mu m}$, the surface tension was estimated: $\gamma\approx 1.1\cdot10^{-5}\,\mathrm{J/m^2}$. This value agrees well with that given by Faetti and Palleschi [7] ($\gamma\approx 0.95\pm0.4\cdot10^{-5}\,\mathrm{J/m^2}$).

Finally, the problem of the wavelength selection at a larger voltage than V_c is a more complicated problem

[1] Note that this value calculated using the formula given at the beginning of the section is compatible with the fact that, for $\Delta T=40\,^\circ\mathrm{C}$, the two phases coexist over a temperature interval of $1.5\,^\circ\mathrm{C}$ (see fig. 2), leading to $G=1.5/(30\cdot10^{-6})=5\cdot10^4\,\mathrm{K/m}$.

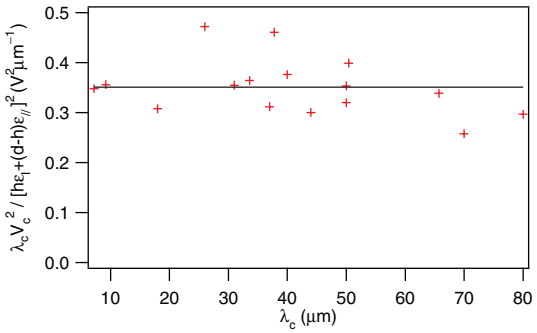

Fig. 9: (Colour on-line) $\lambda_c V_c^2/[h\varepsilon_I + (d-h)\varepsilon_\parallel]^2$ as a function of λ_c. This graph collects data obtained with very different temperature gradients and thicknesses of the nematic layer ($\Delta T = 10$, 20 and 40 °C and $1\,\mu\text{m} < h < 29\,\mu\text{m}$).

because the observed wavelength depends on the dynamics of the process involved. In our case, two hypotheses are possible:

1) Either the interface deforms via a growth and melting process. If the interface velocity is proportional to the energy difference between the two phases (linear kinetics), the fastest mode is also that which minimizes the energy $f(k, G, V)$. This gives immediately by setting the tanh terms equal to 1 in f:

$$\frac{\lambda}{\lambda_c} = \frac{V_c^2}{V^2}. \tag{9}$$

2) Or the deformation is mediated by a hydrodynamic flow. In this case, we should be in the so-called "thin viscous regime" where the growth rate is proportional to $-k^2 f(k, G, V)$ [20]. Because of this dependence, the observed mode is no longer that of minimum energy but that of maximum $-k^2 f(k, G, V)$. This criterion yields

$$\frac{\lambda}{\lambda_c} = \frac{4}{3}\frac{V_c^2}{V^2 + \sqrt{V^4 - (8/9)V_c^4}}, \tag{10}$$

by setting again the tanh terms equal to 1 in f.

But the experimental curves $\lambda(V)$ are much better fitted by eq. (9) than by eq. (10) (their fits to eq. (9) are shown in solid line in the two graphs of fig. 6). This could mean that the interface dynamics is not governed by a hydrodynamic flow, but rather by a melting-freezing process as in the case of the crystallization waves at the ^{4}He solid-liquid interface [21].

Perspectives. – In the future, it would be important to understand why the temperature gradient has such a small stabilizing effect. This is puzzling and deserves further theoretical investigation. The way the interface deforms is also poorly understood. Our analysis suggests that a freezing-melting process rather than a hydrodynamic flow is involved, but this remains to be proved more rigorously by studying in more detail the interface kinetics and its coupling with the macroscopic heat diffusion. Concerning this point, it would be important to measure the instability growth rate as a function of the voltage and to characterize its divergence close to V_c. The role of impurities should also be investigated because they certainly couple to the instability. Finally, it would be interesting to map out the complete phase diagram, in particular at large voltages when the interface behavior becomes non-stationary or chaotic. New experiments to address these issues are in progress.

* * *

A. Dequidt is acknowledged for fruitful discussions and his help in calculating the electric energy using Mathematica.

REFERENCES

[1] de Gennes P. G., *The Physics of Liquid Crystals* (Clarendon, Oxford) 1974.
[2] Faetti S. and Palleschi V., *J. Phys. (Paris)*, **46** (1985) 415.
[3] Yokoyama H., Kobayashi S. and Kamei H., *Mol. Cryst. Liq. Cryst.*, **129** (1985) 109.
[4] Raghunathan V. A., *Phys. Rev. E*, **51** (1995) 896.
[5] Melcher J. R., *Field-Coupled Surface Waves* (MIT Press, Cambridge, Mass.) 1963.
[6] Saville D. A., *Annu. Rev. Fluid Mech.*, **29** (1997) 27.
[7] Faetti S. and Palleschi V., *Phys. Rev. A*, **30** (1984) 3241.
[8] Oswald P. and Pieranski P., *Nematic and Cholesteric Liquid Crystals: Concepts and Physical Properties Illustrated by Experiments* (Taylor & Francis, CRC press, Boca Raton) 2005.
[9] Press M. J. and Arrortt A. S., *Phys. Rev. A*, **8** (1973) 1459.
[10] Oswald P. and Dequidt A., *Phys. Rev. Lett.*, **100** (2008) 217802.
[11] Bradshaw M. J., Raynes E. P., Bunning J. D. and Faber T. E., *J. Phys. (Paris)*, **46** (1985) 1513.
[12] Ratna B. R. and Shashidhar R., *Pramana*, **6** (1976) 278.
[13] Devitt E. B. and Melcher J. R., *Phys. Fluids*, **8** (1965) 1193.
[14] Roberts S. A. and Kumar S., *J. Fluid Mech.*, **631** (2009) 255.
[15] Schäffer E., Thurn-Albrechet T., Russel T. P. and Steiner U., *Nature*, **403** (2000) 874.
[16] Schäffer E., Thurn-Albrechet T., Russel T. P. and Steiner U., *Europhys. Lett.*, **53** (2001) 518.
[17] Mottram N. J., Care C. M. and Cleaver D. J., *Phys. Rev. E*, **74** (2006) 041703.
[18] Lelidis I. and Durand G., *J. Phys. II*, **6** (1996) 1359.
[19] Onuki A., *Physica A*, **221** (1995) 38.
[20] Néron de Surgy G., Chabrerie J.-P., Denoux O. and Weisfreid J.-E., *J. Phys. II*, **3** (1993) 1201.
[21] van Saarloos W. and Weeks J. D., *Phys. Rev. Lett.*, **74** (1995) 290.